

Statistical Ratio Rank Ordered Differences Filter for SeaWiFS Impulse Noise Removal

Zhengjun Liu, Changyao Wang, Aixia Liu, and Xiangming Xiao

Abstract

Due to the 10-bit design of SEAWIFS instrument and the signal transmission, many SEAWIFS satellite images are expected to have lower digitization noise and corrupted impulse noise. In this paper, we first analyze the characteristics of impulse noise and propose a new rank-ordered filter based on the difference of sequence for mean/standard, which is named as Statistical Ratio Rank Ordered Differences (SRROD) filter. Second, we describe the impulse noise detection and removal algorithm in detail. Compared with the median filter and other existing filters, the SRROD filter could effectively remove impulse noises while preserving other valid pixels without, or only with minor, modification. Through adjusting the lower and upper threshold values, different filter performance could be achieved. We also discuss the blind parameters optimization for non-recursive implementation. Based on the assessment of the distribution map of performance estimator ε according to different lower and upper threshold pairs, a nearly optimal threshold could be obtained. Finally, some concluding remarks are also presented in this paper.

Introduction

During remote sensing image acquisition, transmission, and processing, due to the limitation of instrumental design, environmental and atmosphere conditions, channel transmission errors, signal encoding processing, and other reasons, images can be corrupted by some stochastic and randomly distributed black and white noises, which are usually called *impulse noise*, or *salt and pepper noise*. Salt and pepper noises severely degrade the image quality and limit quantitative assessment. Therefore, noise removal is very important for remote sensing imagery and other image processing, and it is also significant in improving the resultant effect of image segmentation, feature extraction, image recognition, and classification.

At present, image filtering is the main method for removing noises from an image. The goal of impulse noise removal is to suppress the noise while preserving the integrity of edges and detail information. Conventional linear filters, such as mean filters, are not very effective for the removal of

salt and pepper noise; while some nonlinear filters, for example, the median filter (Turky, 1971; Lin and Willson, 1988) and order statistic (OS) filters (Kim, 1986, 1995; Bovik, 1983), can efficiently reduce most of the salt and pepper noise in the image with its edges and texture information degraded to varying degrees. Another limitation is the robustness of these algorithms; that is, the performance of the algorithms decreases significantly when the percentage of impulse noise in the image increases. To overcome this problem, some new algorithms have been recently proposed: the multistage median filters (Wendt *et al.*, 1986; Coyle *et al.*, 1988, 1989; Lin *et al.*, 1990), center weighted median (CWM) filters (Hardie *et al.*, 1993; Ko *et al.*, 1991; Sun *et al.*, 1992), general weighted median (WM) filters and weighted order statistic (WOS) filters (Yli-Harja *et al.*, 1991), length adaptive median filter (Lin and Willson, 1988), decision-based median filter (Florencio and Schafer, 1994), stack filters (Coyle *et al.*, 1988, 1989; Lin *et al.*, 1990; Wendt *et al.*, 1986), permutation filters (Barner *et al.*, 1994), and rank-conditioned, rank-selection filters (Hardie, 1994). Most of these filters have demonstrated better performance than the median filter in the removal of impulse noise and detail preservation. However, because most of these approaches are typically implemented uniformly across an image, they also tend to modify pixels that are undisturbed by noises. In addition, some researchers introduced impulse noise filter using fuzzy logic techniques (Zhang and Wang, 1997; Wang and Zhang, 1998). These algorithms are based on fuzzy impulse detection and fuzzy noise cancellation techniques. Although there is some effective improvement, there are still difficulties to create the fuzzy rule like other fuzzy systems, especially when no training images are provided.

In this paper, a novel, non-linear, adaptive algorithm is proposed for the removal of impulse noise from SEAWIFS images. The paper is organized as follows: the mathematical model of random-valued impulse noise is described; the detailed algorithm and image-processing technique based on Statistical Ratio Rank Ordered Differences (SRROD) filter is studied; the experimental results of applying our filter to SEAWIFS impulse noise removal is discussed; a non-iterative optimization of filter parameters is discussed; and finally, the conclusion.

Impulse Noise Model and Algorithm Consideration

Normally, impulse noise is a result of a random process in which the digital numbers (DNs) of the corrupted pixels are

Z. Liu, C. Wang, and A. Liu are with the Laboratory of Remote Sensing Information Science, Institute of Remote Sensing Applications, CAS, Beijing 100101, China (zjliu@casm.ac.cn).

Z. Liu is also with the Institute for Photogrammetry and Remote Sensing, Chinese Academy of Surveying and Mapping, No.16 Beitaiping Road, Beijing 100039, China.

X. Xiao is with the Complex System Research Center, Institute for the Study of Earth, Oceans, and Space, University of New Hampshire, Durham, NH 03824-3525.

Photogrammetric Engineering & Remote Sensing
Vol. 71, No. 1, January 2005, pp. 89–95.

0099-1112/05/7101-0089/\$3.00/0
© 2005 American Society for Photogrammetry
and Remote Sensing

often replaced with values equal to or near the minimum or maximum value of the allowable dynamic range. The noises could be positive (maximum), negative (minimum), or a mixture (salt and pepper). Pixels are degraded by such noises with probability p . Assuming the original noise-free image value at pixel location $\mathbf{n} = [i, j]$ is $v(\mathbf{n})$, and $x(\mathbf{n})$ is the observed noise degraded image value, the noise model is expressed as:

$$x(\mathbf{n}) = \begin{cases} e(\mathbf{n}), & \text{with } p \\ v(\mathbf{n}), & \text{with } 1-p \end{cases} \quad (1)$$

where $e(\mathbf{n})$ is a random binary number. For an 8-bit, gray scale image representation (0 = minimum; 255 = maximum), its value is

$$e(\mathbf{n}) = \begin{cases} 0, & \text{with } p_0 \\ 255, & \text{with } 1-p_0 \end{cases} \quad (2)$$

The probability of the black (minimum) value is p_0 and the probability of the white (maximum) value is $1-p_0$. Normally, for positive impulse, $p_0 = 0$; for negative impulse, $p_0 = 1$; and for the salt and pepper, $p_0 = 1/2$. Any mixture of black and white can be obtained by a different selection of the probability p_0 .

More complex impulse noise models are generated by a random magnitude degradation procedure. The random-valued impulse noise $e(\mathbf{n})$ is represented as:

$$i = z(n) \quad i \in \{1, 2, 3, \dots\} \quad (3)$$

$$e(\mathbf{n}) = s_i(\mathbf{n})$$

where the impulse generation function $s_i(\mathbf{n})$ is a set of random processes representing an ever-present impulse component with standard deviation σ_i , and $z(n)$ is a random unsigned integer value selected at pixel location \mathbf{n} . For a specific example, $s_i(\mathbf{n})$ could be a series of normal distributions with different means and standard deviations, and could be represented as:

$$s_i(\mathbf{n}) = p_i(t) = N(\mu_i, \sigma_i^2) = \frac{1}{\sigma_i \sqrt{2\pi}} e^{-\frac{(t-\mu_i)^2}{2\sigma_i^2}} \quad i = 1, 2, \dots, n \quad (4)$$

where $\{p_i(t)\}$ are the set of normal distribution functions $N(\mu_i, \sigma_i^2)$ with mean value μ_i and standard deviation σ_i , and t is the random noise variable. Normally, t is constrained in a narrow extent compared to the full allowable range of data value of an image. Note that the mixture of the signals and various types of noise makes a single threshold applying in noise-disturbed image to the removal of impulse noise is not desirable.

As aforementioned, the goal of impulse noise removal is to suppress the noise while preserving the edges and structure or texture information. More strictly, in many remote sensing applications, especially in quantitative remote sensing retrieval and image classification, users generally expect that impulse noise can be removed as much as possible while preserving the undisturbed pixels without modification. Therefore, to assess the effectiveness of the proposed impulse noise removal algorithm, three factors (percentage of the impulse noise removed, the edge and texture preservation, and pixel value modification) should be considered and compared. In addition, the algorithm complicity, computational speed, and efficiency are the other factors to consider.

In the next section, we will introduce a novel non-linear adaptive algorithm for removal of impulse noise from the image and minimizing undisturbed pixel modification that helps preserve edges, structure, and texture information.

Algorithm Implementation and Experimental Results

Design Strategies

This algorithm first sorts pixel-by-pixel similar to some rank ordered filters in a local window. Then, a sequence of local statistics based on the mean values and standard deviations in the local window are calculated, sequentially subtracted, and compared with two predefined thresholds: i.e., a lower threshold employed for black noise detection and an upper threshold employed for white noise detection. If noise is detected, the pixel value is modified and replaced by rank-ordered mean (Abreu, 1996) or other appropriate local window statistics as described below.

Let $v(\mathbf{n})$, $x(\mathbf{n})$, and $y(\mathbf{n})$ represent the pixel values of the original noise-free image, the impulse-noise-corrupted image, and the filtered output image, respectively. The impulse noise removal scheme of our proposed algorithm could be summarized as the following steps:

- (1) First, consider the real-valued 2D sequence $\{x(\mathbf{n})\}$, and define $X(\mathbf{n})$ as a $w \times w$ element observation vector that contains the elements of a $w \times w$ window centered around $x(\mathbf{n})$ such as $X(n) = [x_i(n); (i = 1, 2, \dots, w^2)]$. In this case, the $x_i(\mathbf{n})$ s correspond to a left-to-right, top-to-bottom mapping from the $w \times w$ window to the 1D vector. The observation samples can be also ordered by rank, which defines the vector $R(n) = [r_i(n); (i = 1, 2, \dots, w^2)]$, where $r_i(n)$ are the elements of $X(n)$ arranged in a descent order such that $r_1(n) \geq r_2(n) \geq \dots \geq r_{w^2}(n)$.
- (2) Next, denote $R_{p \rightarrow q}(n) = [r_i(n); (i = p, p+1, \dots, q-1, q)]$ as a subset sequence in vector R with its elements coming from $r_p(n)$ to $r_q(n)$, where $1 \leq p < q \leq w^2$. The iterative computation of the downward differences of the ratios between the truncated mean values and the standard deviations, denoted as $\{K_i\}$, is based on the following equations:

$$\mu(R_{p \rightarrow q}(n)) = \frac{1}{q-p+1} \sum_{i=p}^q r_i(n), \quad (5)$$

$$\begin{aligned} \sigma(R_{p \rightarrow q}(n)) &= \sqrt{D(R_{p \rightarrow q}(n))} \\ &= \sqrt{\mu\{[R_{p \rightarrow q}(n) - \mu(R_{p \rightarrow q}(n))]^2\}} \\ &= \sqrt{\mu(R_{p \rightarrow q}^2(n)) - (\mu(R_{p \rightarrow q}(n)))^2}, \text{ and} \end{aligned} \quad (6)$$

$$K_i = \left| \frac{\sigma(R_{1 \rightarrow (w^2-i)}(n))}{\mu(R_{1 \rightarrow (w^2-i)}(n))} - \frac{\sigma(R_{1 \rightarrow (w^2-i-1)}(n))}{\mu(R_{1 \rightarrow (w^2-i-1)}(n))} \right| \bigg/ \frac{\sigma(R_{1 \rightarrow w^2}(n))}{\mu(R_{1 \rightarrow w^2}(n))}, \quad (7)$$

$$0 \leq i \leq \frac{w^2-1}{2}$$

where $\mu(R_{p \rightarrow q}(n))$, $D(R_{p \rightarrow q}(n))$, $\sigma(R_{p \rightarrow q}(n))$ are the mathematical expectation, variance and standard deviation for 1D rank ordered subset sequence $R_{p \rightarrow q}(n)$, respectively.

The reason for applying a normalization in Equation 7 is that the varying characteristics of local structures over the whole image could not be captured by one global function. By employing the normalization, one can remove the shiftiness effects of pixel values.

- (3) Compare K_i with a predefined or specified lower threshold C_l , ($C_l \in R^+$, namely, C_l is a positive float-valued constant, and in most cases we have $C_l \in [0, 1.0]$). If $K_i > C_l$, the pixel values with subscript ranging from i to w^2 in vector $R(n)$, that is, $r_i(n), r_{i+1}(n), \dots, r_{w^2}(n)$, will be detected as black noises. Let k denote the total number of black noises in current local window centered around pixel \mathbf{n} , in which we will have $0 \leq k \leq \frac{w^2-1}{2}$ from Equation 7; if no noise presents, simply let $k = 0$.
- (4) Similar to Step 2 above, compute the normalized upward differences of the ratios between the truncated mean values and the truncated standard deviation by using the following equation, and denote this upward sequence as $\{L_i\}$:

$$L_i = \left| \frac{\sigma(R_{i \rightarrow (w^2-k+1)}(n))}{\mu(R_{i \rightarrow (w^2-k+1)}(n))} - \frac{\sigma(R_{(i+1) \rightarrow (w^2-k+1)}(n))}{\mu(R_{(i+1) \rightarrow (w^2-k+1)}(n))} \right| \bigg/ \left[\frac{\sigma(R_{1 \rightarrow (w^2-k+1)}(n))}{\mu(R_{1 \rightarrow (w^2-k+1)}(n))} \right], \quad (8)$$

$$0 \leq i \leq \frac{w^2-1}{2}$$

- (5) Compare L_i with predefined or specified upper threshold C_u , ($C_u \in R^+$, namely, C_u is a positive real number constant, and in general, $C_u \in [0, 1]$). If $L_i > C_u$, the pixel values with subscript from 1 to i in vector $R(n)$, that is, $r_1(n), r_2(n), \dots, r_i(n)$, will be detected as black noises. Let l denote the total number of black noises in current local window centered around pixel \mathbf{n} , in which we will have $0 \leq l \leq \frac{w^2-1}{2}$ from Equation 8; if no noise results, simply let $l = 0$;
- (6) Determine whether the center pixel \mathbf{n} in local window is noise pixel or not by using Equation 9. If an impulse noise is detected, replace it with its rank-ordered mean (ROM) value or other localized estimation:

$$y(n) = \begin{cases} x(n) & \text{if } r_{w^2-k+1}(n) < x(n) < r_l(n) \\ \mu(R_{l \rightarrow (n^2-k+1)}(n)) & \text{if } x(n) \geq r_l(n) \text{ or } x(n) \leq r_{w^2-k+1}(n). \end{cases} \quad (9)$$

For highly corrupted images, median of $R_{l \rightarrow (n^2-k+1)}$ may be preferable.

- (7) Move the window to the next pixels from left to right and from top to bottom according to the Steps from 1 to 6 until all pixels in noisy image are processed, and the final filtered output image, $y(\mathbf{n})$, is obtained.

The filtering algorithm described here works well in either a non-recursive or recursive implementation. In recursive fashion, a higher valued threshold pair than non-recursive implementation should be given, resulting in less noise removal and less pixel modification in each iteration, but better noise removal and detailed information preservation in the final result. Meanwhile, users can change the upper threshold and lower threshold and the local window size in each iteration if necessary, so that optimal filtering result may be achieved.

Comparative Experiment on Natural Images

We evaluated the proposed method with an 8-bit, 256×256 test image ("Lena") shown in Figure 1a corrupted at the rate from 5 percent to 20 percent. Figure 1b and 1c show the corrupted image with 15 percent random-valued impulse noise and the restored image by our filtering method, respectively.

Three previously published algorithms including the median filter, the standard two-state non-recursive SD-ROM filter (Abreu *et al.*, 1996) and the decision-based filter (Florencio and Schafter, 1994) are incorporated for comparison. As performance measures, we used the peak signal-to-noise ratio (PSNR) with a unit of decibel (DB), the mean absolute error (MAE), and the percent pixels modification (PPM) defined as:

$$PSNR = 10 \log_{10} \left(\frac{\sum_{n=1}^N G^2}{\sum_{n=1}^N (y(n) - x(n))^2} \right), \quad (10)$$

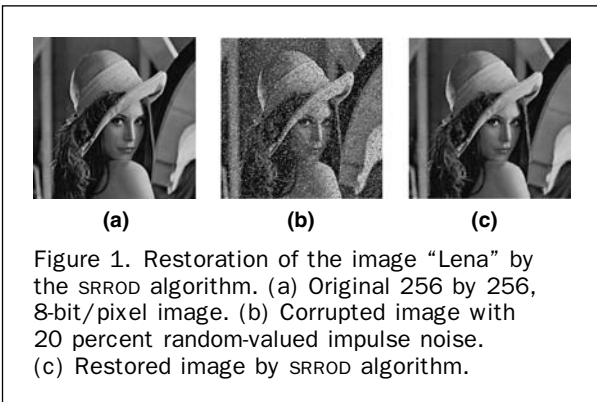


TABLE 1. COMPARATIVE RESTORATION RESULTS IN PSNR, MAE AND PPM AT DIFFERENT RATES OF RANDOM-VALUED IMPULSE NOISE

Algorithm	Factors	Percentage of Impulse Noise			
		5%	10%	15%	20%
Median	PSNR	31.02 dB	29.74 dB	28.74 dB	28.08 dB
	MAE	3.31	3.93	4.4	4.87
	PPM	65.07%	68.78%	70.78%	72.63%
SD-ROM ¹	PSNR	29.66 dB	28.31 dB	27.46 dB	27.01 dB
	MAE	3.44	4.58	5.26	6.01
	PPM	38.47%	55.67%	63.86%	72.13%
Decision-based Median ²	PSNR	32.35 dB	29.86 dB	28.06 dB	27.72 dB
	MAE	1.73	3.54	4.6	3.92
	PPM	23.01%	54.69%	62.51%	33.72%
SRROD filter ²	PSNR	32.68 dB	30.23 dB	29.21 dB	28.75 dB
	MAE	1.68	2.91	3.37	3.23
	PPM	25.04%	39.10%	46.33%	37.76%

¹implemented two state approach with recommended standard thresholds.

²implemented recursively at 20 percent impulse noise.

$$MAE = \frac{\sum_{n=1}^N |y(n) - x(n)|}{N}, \text{ and} \quad (11)$$

$$PPM = \frac{N_0}{N} \times 100\% \quad (12)$$

where N is the total number of pixels in an image, N_0 is the number of pixels with DN changed, and G is the maximum allowable data value for the image pixels. A good noise removal algorithm should have relatively high PSNR, low MAE, and low PPM.

Table 1 lists the comparative results of our experiment. All algorithms are implemented using a 3×3 window. Clearly, our filter provides significant improvement over the other tested methods for random-valued impulse noise. Note that the decision-based median filter and our filter are implemented recursively for 20 percent impulse noise removal. Interestingly, significant decrease of PPM and little loss of MAE and PSNR are acquired for our filter than the non-recursive implementation for 15 percent impulse noise. This may imply that a carefully designed, recursive implementation of our filter could maximize the filtering performance.

Application in SEAWIFS Noise Removal

A 1285×1616 , 8-channel SEAWIFS image corrupted by impulse noise in East Asia obtained on 05 January 2001 is used for our experiment and subjective evaluation. The nominal spatial resolution is 1.1 km for all bands. For simplicity, only Channel 2 is selected for visualization and assessment in this paper. Different filtering results compared between our algorithm, median filter, and decision-based median filter are illustrated in Figure 2. Similar results are also obtained in other channels but will not be discussed here.

Figure 2a shows an enlarged original Level 1B image of SEAWIFS products corrupted with evident impulse noise. Visualization of the full scene image shows that the impulse noise is random and inhomogeneous in a small area, but approximately more homogeneous in a larger area. Noise density can reach over 30 percent in some small local windows while in other areas only a few new noises or no noise may be found. The overall average noise probability

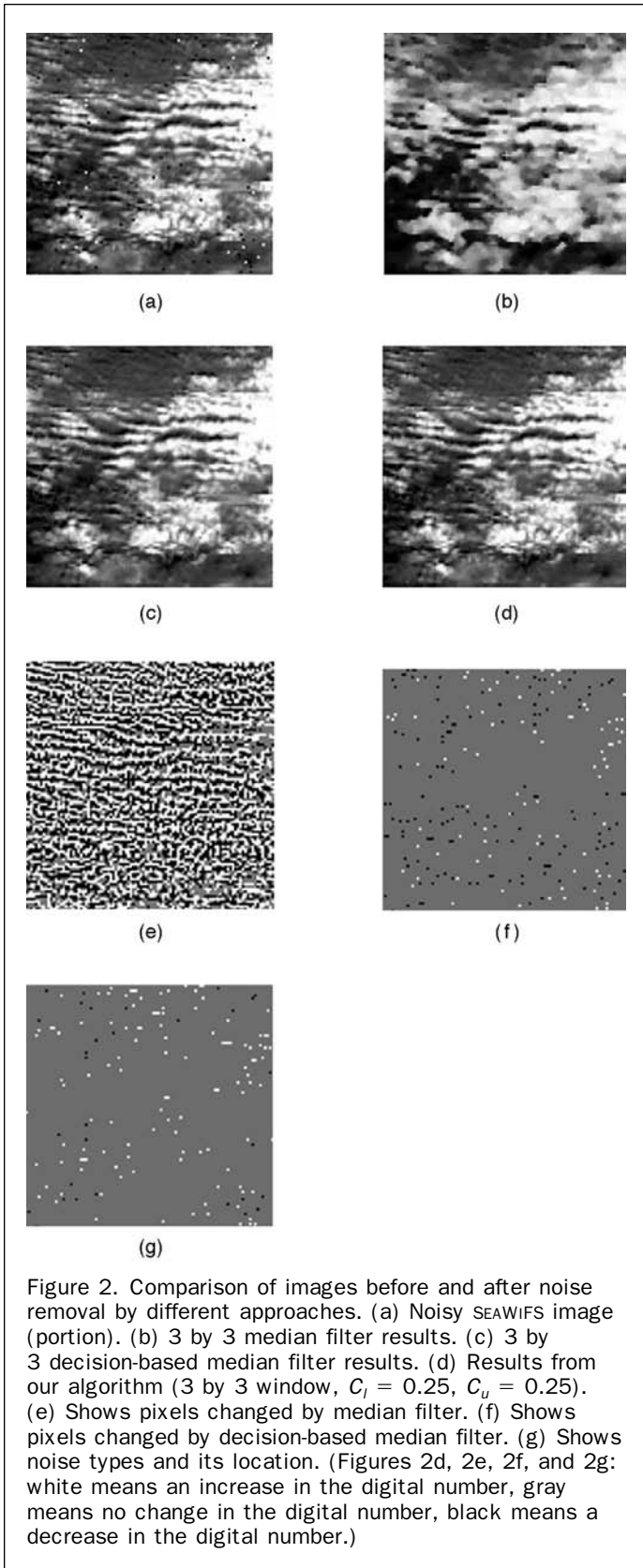


Figure 2. Comparison of images before and after noise removal by different approaches. (a) Noisy SEAWIFS image (portion). (b) 3 by 3 median filter results. (c) 3 by 3 decision-based median filter results. (d) Results from our algorithm (3 by 3 window, $C_l = 0.25$, $C_u = 0.25$). (e) Shows pixels changed by median filter. (f) Shows pixels changed by decision-based median filter. (g) Shows noise types and its location. (Figures 2d, 2e, 2f, and 2g: white means an increase in the digital number, gray means no change in the digital number, black means a decrease in the digital number.)

may be lower than 10 percent. Figure 2b shows the median filtering result for the image in Figure 2a. From Figure 2b we can see that, although the impulse noise can be fully

removed from the image, the texture and edge information has also been severely blurred. From Figure 2c we can see that the decision-based, median filter performs much better than the median filter, although some undisturbed pixels are also classified as impulse pixels, which we will discuss in the next paragraph. The image shown in Figure 2d is the final result filtered by our approach. This is performed within a 3×3 window size, and with $C_l = 0.25$, $C_u = 0.25$. Compared Figure 2d with Figure 2a–c, we find that our method can not only successfully remove nearly all of the impulse noise, but most importantly, preserves its texture and edge information perfectly.

By subtracting the filtered image from the original image, we obtain the *difference image* before and after filtering. Thus, we can analyze changes of pixel values between original and filtered images. Figure 2e shows the difference image obtained by subtracting original image (Figure 2a) from the median filtering resulted image (Figure 2b); while the difference image shown in Figure 2f and g are obtained by subtracting original image from the filtering result image by using the decision-based median (Figure 2c) and the method proposed in this paper (Figure 2d), respectively. In these difference images the medium gray pixels represent the unchanged pixels after noise removal; white represents pixels with increased data value; and black represents pixels with decreased data value. Figure 2e demonstrates the dramatic, altered data values almost for most of the pixels in original image by median filtering; however, images illustrated in Figure 2f and 2g show that almost all impulse noises are removed with only a few altered pixels by both the decision-based, median filter and our approach. Manual verification of Figure 2f and 2g shows that some of the undisturbed bright pixels are misclassified as white noisy pixels by the decision-based median filter; this situation rarely occurs in the filtered image by our approach. Therefore, Figure 2g well delineates the location, characteristics, and intensity of impulse noises of the original image, where white indicates the occurrence of black noises and black indicates the occurrence of white noises in original image.

Figure 3a and 3b show histograms of the images before and after noise removal using the algorithm discussed in this paper. Note that in Figure 3, the impulse noises are mainly distributed in places where data values (or digital number, DN) are less than 450 or more than 800. By comparing the histograms in Figure 2a and 2b, we can see that after noises being removed from original image, the dramatically decreased frequency of these DNs in these two regions contributes to the increase of frequency centered around the data value 500.

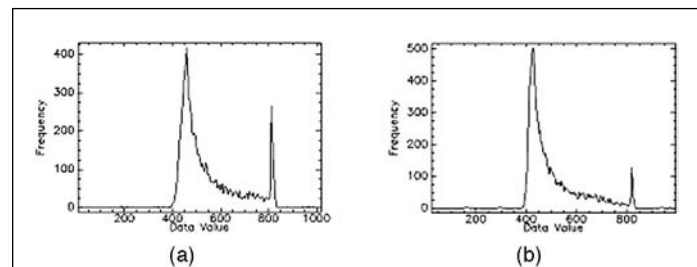


Figure 3. Changes of histograms before and after noise removal for image in Figure 2a. (a) Histogram before noise removal. (b) Histogram after noise removal.

Blind Parameters Optimization for Non-Recursive Implementation

In this section, we will address the parameters optimization without training data for non-recursive implementation of our proposed filter. This procedure can be applied on all SEAWIFS imagery in general, except that the values of specific parameters may depend on the quality of the individual image.

From the histogram shown in Figure 3a, we notice that most impulse noises in the image are distributed between the minimum and maximum pixel values, clustered at different locations as separated “peaks” with different amplitudes and different widths. Although we cannot delineate noises and their locations from signals according to the histogram, we can easily approximate these peaks by using Equations 3 and 4 described in the noise modeling section. Under this assumption, we will begin to discuss the optimization of the thresholds (C_l , C_u).

First, in order to estimate the filtering performance concerning different (C_l , C_u) values when the original noise free image is not available, we have developed a quantitative indicator ε which is defined as:

$$\varepsilon = \begin{cases} 10 \cdot \log_{10} \frac{G^2}{\frac{1}{N-N_0} \sum_{n=1}^N (y(n)-x(n))^2} & \text{if } N \neq N_0; \\ 0 & \text{if } N = N_0. \end{cases} \quad (13)$$

where N_0 is the number of pixels that the DN changed. Generally, the larger the value of ε , the better the denoising efficiency and the less pixel value modification results, provided that most noises have been removed from the noisy image; or vice versa. For simplicity, let's denote function $\varepsilon(cl, cu)$ as the estimated ε for given lower threshold and upper threshold (C_l , C_u).

Then, a 400×400 subset portion of the degraded SEAWIFS image from Channel 2 is chosen as the training sample image. Our experiment shows that this size of image is an ideal compromise between the noise characteristics of the full scene image and computational complexity. Next, we calculate the $\varepsilon(cl, cu)$ values of input sample image after each iteration of filtering operation according to various (C_l , C_u) values ranging from [0, 0.5] at a 0.05 sampling interval. After that, we will have a two-dimensional $\varepsilon(cl, cu)$ matrix according to different (C_l , C_u) values. The $\varepsilon(cl, cu)$ matrix are then bilinearly interpolated and are plotted as an $\varepsilon(cl, cu)$ distribution map overlaid with contour lines shown in Figure 4a. Note that the horizontal coordinate represents

the lower threshold C_l , while the vertical coordinate represents the upper threshold C_u .

Note in Figure 4a we have some abruptly skewed contour lines exhibited as rows or columns of strips distributed on the $\varepsilon(cl, cu)$ distribution map, which are respectively labeled as 1, 2, 3 for up-down strips, and a, b, c for left-right strips. To look closer to these specific strips, the $\varepsilon(cl, cu)$ are recalculated with 0.01 cl , cu 's sampling interval, and cl 's values ranging from [0.05, 0.2], cu 's values ranging from [0.1, 0.3]. Figure 4b is the resulting fine detailed $\varepsilon(cl, cu)$ distribution map. We can still find the up-down and left-right stripes in this figure.

This result could be interpreted from two aspects. First, since our algorithm is developed based on the iterative estimation of the normalized local window statistics, any exception beyond an ordinary neighborhood statistics will be detected and treated as noise factors, in which this feature will not be influenced by the absolute pixel values; Second, due to the globally clustered characteristic of noises in the SEAWIFS image, equally changed (C_l , C_u) values will not surely result in equal quantity of noise being detected. Therefore, those strip locations could be normally explained as where the most impulse noise have been removed and implied, where the impulse noise clustered. Accordingly, the crosses between those up-down strips and the left-right strips are where the most black and white impulses are removed. If we set the (C_l , C_u) values to lower-left corner at these crosses, we can have more impulse noises removed and with less amount of ordinary pixels misclassified as noises, preserving the image content with little influence.

To accurately locate the optimized thresholds, we apply a C_l and C_u partial differential and second order differential (Laplacian Operator) (Castleman, 1996) to $\varepsilon(cl, cu)$ and overlay it with contour lines shown in Figure 4a and 4b. The Laplacian transform equation is given by Equation 14:

$$\frac{\partial^2 \varepsilon}{\partial cl^2} + \frac{\partial^2 \varepsilon}{\partial cu^2} \approx 4\varepsilon(cl, cu) - [\varepsilon(cl+1, cu) + \varepsilon(cl-1, cu) + \varepsilon(cl, cu+1) + \varepsilon(cl, cu-1)] \quad (14)$$

which corresponds to the 3×3 convolution operator $p(cl, cu)$ in Equation 15:

$$p(cl, cu) = \begin{bmatrix} 0 & -1 & 0 \\ -1 & 4 & -1 \\ 0 & -1 & 0 \end{bmatrix}. \quad (15)$$

The results are illustrated in Figure 5a–f.

In Figure 5a and 5b we can see that, the up-down strips in Figure 4a and 4b are shown as densely clustered, nearly straight up-down contour lines; the left-right strips in Figure 4c and 4d are also shown as densely clustered, nearly straight left-right contour lines in Figure 5c and 5d. Those crosses shown in Figure 4a and 4b are exhibited as points with contour lines clustered and interlaced together in Figure 5e and 5f. Those lower-left points close to these points are the possible point candidates for optimized thresholds, as we have marked out in Figure 5f. Careful evaluation confirms that when (C_l , C_u) is set to (0.125, 0.275) for this scene of the Channel 2 image, best filtering results can be achieved.

Figure 6 shows the full image size processing result using the optimized threshold pair acquired from subset training image. It provides a good solution to remove the impulse noises from the image while preserving the texture and edge information of image, as well as, keeping the digital number of the undisturbed pixels without or only with a little change.

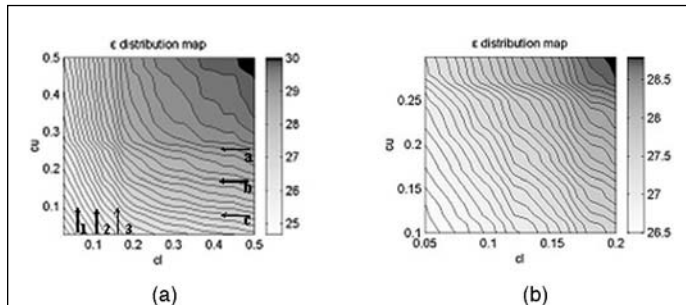


Figure 4. $\varepsilon(cl, cu)$ distribution map overlaid with contour lines (Unit: dB). (a) Sampling interval: 0.05, range: [0, 0.5]. (b) Sampling interval: 0.01, range: cl is [0.05, 0.2], cu is [0.1, 0.3].

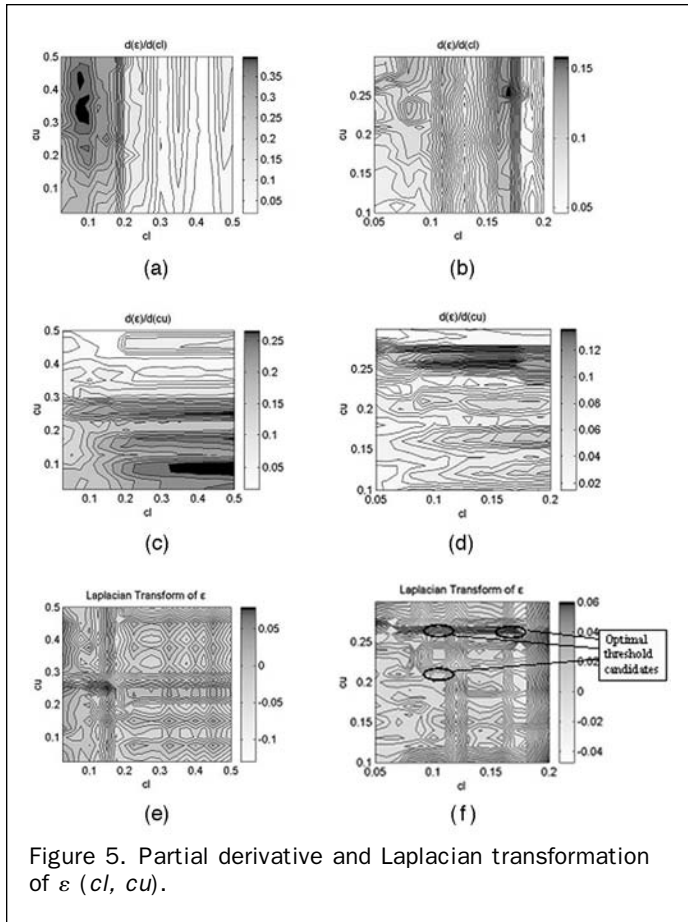


Figure 5. Partial derivative and Laplacian transformation of ε (cl , cu).

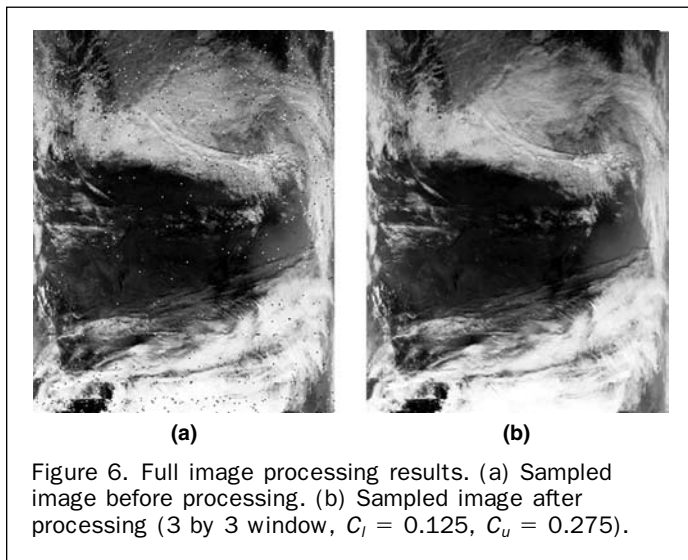


Figure 6. Full image processing results. (a) Sampled image before processing. (b) Sampled image after processing (3 by 3 window, $C_l = 0.125$, $C_u = 0.275$).

Conclusion

In this paper, a non-linear, adaptive filter to remove impulse noises from the remote sensed image has been presented. The key point of the algorithm is to sort the pixel values, to compute the sequences of standard deviations and means, and then, to utilize the normalized differences between two successive standard deviation/mean ratios. Noise detection

is achieved by thresholding these differences. Noise suppression is achieved by replacing the pixel value with the rank-ordered mean. The algorithm has been tested on simulated data and a real SEAWIFS image so that its creditability is established. By considering the generalized impulse noise model discussed in the paper, we analyzed the quantitative relationship between the noise removal performance and the threshold parameters. Finally, the strategy for retrieval of the optimized thresholds has also been presented for non-recursive implementation. These gains can be observed in terms of both the visual examination and the quantitative assessment of the restored images.

Acknowledgments

The authors would like to thank the SEAWIFS Project (Code 970.2) and the Distributed Active Archive Center (Code 902) at the Goddard Space Flight Center, Greenbelt, MD 20771 for the production and distribution of SEAWIFS data, respectively. The authors also greatly appreciate the support by the International Cooperation Key Project of Ministry of Science and Technology, China (2001DFBA0005), the China's Special Funds for Major State Research Project (G2000077900), and the Knowledge Innovation Program of the Chinese Academy of Sciences (KZCX1-SW-01).

References

- Abreu, E., M. Lightone, and S.K. Mitra, 1996. A new efficient approach for the removal of impulse noise from highly corrupted images, *IEEE Transactions on Image Processing*, 5(6):1012–1025.
- Barner, K., and G.R. Arce, 1992. Permutation filters: A class of nonlinear filters based on set permutations, *IEEE Transactions on Signal Processing*, 42(4):782–798.
- Bovik, A.C., T. Huang, and D.C. Munson, 1983. A generalization of median filtering using linear combinations of order statistics, *IEEE Transactions on Acoustical Speech Signal Processing*, 31:1342–1350.
- Brownrigg, D.R.K., 1984. The weighted median filter, *Communications of the Association for Computing Machinery*, 27: 807–818.
- Castleman, K.R., 1996. *Digital Image Processing*, Prentice Hall, Inc., Upper Saddle River, New Jersey.
- Coyle, E.J., and J.H. Lin, 1988. Stack filters and the mean absolute error criterion, *IEEE Transactions on Acoustical Speech Signal Processing*, 36(8):1244–1254.
- Coyle, E.J., J.H. Lin, and M. Gabbouj, 1989. Optimal stack filtering and the estimation and structural approaches to image processing, *IEEE Transactions on Acoustical Speech Signal Processing*, 37(12):2037–2066.
- Florencio, D.A.F., and R.W. Schafer, 1994. Decision-based median filter using local signal statistics. *Proceedings from SPIE Symposium on Visual Communications in Image Processing*, Chicago, pp. 268–275.
- Hardie, R.C., and C.G. Boncelet, 1993. LUM filters: A class rank order based filters for smoothing and sharpening, *IEEE Transactions on Signal Processing*, 41(3):1061–1076.
- Hardie, R.C., and K.E. Barner, 1994. Rank conditioned rank selection filters for signal restoration, *IEEE Transactions on Image Processing*, 3(2):192–206.
- Hwang, H., and R. A. Haddad, 1995. Adaptive median filters: new algorithms and results, *IEEE Transactions on Image Processing*, 4(4):499–502.
- Justusson, B.I., 1981. Median filtering: statistical properties, *Two-Dimensional Digital Signal Processing II* (T. S. Huang, editor), Springer Verlag, Inc., Berlin, pp. 161–196.
- Kim, S.R., and A. Efron, 1995. Adaptive robust impulse noise filtering, *IEEE Transactions on Signal Processing*, 43(8):1855–1866.

- Kim, V., and L. Yaroslavskii, 1986. Rank algorithms for picture processing, *Computer Vision, Graphics, Image Processing*, 35(2):234–258.
- Ko, S.J., and Y.H. Lee, 1991. Center weighted median filters and their applications to image enhancement, *IEEE Transactions on Circuits Systems*, 38(9):983–993.
- Lin, H.M., and A.N. Willson, 1988. Median Filters with adaptive length, *IEEE CAS1*, 35(6):675–690.
- Lin, J.H., T.M. Sellke, and E.J. Coyle, 1990. Adaptive stack filtering under the mean absolute error criterion, *IEEE Transactions on Acoustical Speech Signal Processing*, 38(6):938–954.
- Shi, Z., D.S. Zhang, D.J. Kouri, and D.K. Hoffman, Nonlinear Quincunx Filters, *IEEE Transactions on PAMI* (submitted).
- Sun, T., M. Gabbouj, and Y. Neuvo, 1992. Deterministic properties of center weighted median filters, *Proceedings of the 1992 IEEE International Conference for Communication Technology*, Tsinghua Campus, Beijing, China.
- Tukey, J.W., 1971. *Exploratory data analysis*, Addison-Wesley, New York.
- Wang, Z., and D. Zhang, 1998. Restoration of impulse noise corrupted images using long-range correlation, *IEEE Signal Processing Letter*, 5:4–7.
- Wendt, P.D., E.J. Coyle, and N.C. Gallagher, 1986. Stack filters, *IEEE Transactions on Acoustical Speech Signal Processing*, 34(8):898–911.
- Yli-Harja, O., J. Stola, and Y. Neuvo, 1991. Analysis of the properties of median and weighted median filters using threshold logic and stack filter representation, *IEEE Transactions on Signal Processing*, 39(2):395–410.
- You, X., and G. Grebbin, 1995. A robust adaptive estimator for filtering noise in images, *IEEE Transactions on Image Processing*, 4(5):693–699.
- Zhang, D., and Z. Wang, 1997. Impulse noise detection and removal using fuzzy techniques, *Electronics letters*, 33(5):378–379.